SRNL-STI-2009-00184
Rev. 0

IMPACT OF TIME/TEMPERATURE CURING CONDITIONS AND ALUMINATE CONCENTRATION ON SALTSTONE PROPERTIES

J. R. Harbour, T. B Edwards and V. J. Williams

Savannah River National Laboratory

April 2009

Savannah River National Laboratory
Savannah River Nuclear Solutions
Aiken, SC 29808

Prepared for the U.S. Department of Energy Under Contract Number DE-AC09-08SR22470

SRNL
SAVANNAH RIVER NATIONAL LABORATORY

DISCLAIMER

Printed in the United States of America

Prepared For
U.S. Department of Energy

SRNL-STI-2009-00184
Rev. 0

Key Words: *Permeability*
Porosity
Compressive Strength

Retention: Permanent

IMPACT OF TIME/TEMPERATURE CURING CONDITIONS AND ALUMINATE CONCENTRATION ON SALTSTONE PROPERTIES

J. R. Harbour, T. B Edwards and V. J. Williams

Savannah River National Laboratory

April 2009

Savannah River National Laboratory
Savannah River Nuclear Solutions
Aiken, SC 29808

Prepared for the U.S. Department of Energy Under Contract Number DE-AC09-08SR22470

REVIEWS AND APPROVALS

AUTHORS:

J. R. Harbour, SRNL, Engineering Process Development Date

T. B. Edwards, SRNL, Applied Comp Eng & Statistics Date

V. J. Williams, SRNL, Engineering Process Development Date

TECHNICAL REVIEWERS:

A. D. Cozzi, SRNL, Engineering Process Development Date

APPROVERS

A. B. Barnes, SRNL, Manager, Engineering Process Development Date

S. L. Marra, SRNL, Manager, E&CPT Research Programs Date

J. E. Occhipinti, Manager, Waste Solidification Engineering Date

EXECUTIVE SUMMARY

This report addresses the impact of (1) the time and temperature curing conditions (profile) and (2) the impact of higher aluminate concentrations in the decontaminated salt solution on Saltstone processing and performance properties.

The results demonstrate that performance properties as well as some of the processing properties of Saltstone are highly sensitive to the conditions of time and temperature under which curing occurs. This sensitivity is in turn dependent on the concentration of aluminate in the salt feed solution. In general, the performance properties and indicators (Young's modulus, compressive strength and total porosity) are reduced when curing is initially carried out under high temperature. However, this reduction in performance properties is dependent on the sequence of temperatures (the time/temperature profile) experienced during the curing process. That is, samples that are subjected to a 1, 2, 3 or 4 day curing time at 60 °C followed by final curing at 22 °C lead to performance properties that are significantly different than the properties of grouts allowed to cure for 1, 2, 3 or 4 days at 22 °C followed by a treatment at 60 °C. The performance properties of Saltstone cured in the sequence of higher temperature first are generally less (and in some cases significantly less) than performance properties of Saltstone cured only at 22 °C. This loss in performance was shown to be mitigated by increased slag content or cement content in the premix at the expense of fly ash. For the sequence in which the Saltstone is initially cured at 22 °C followed by a higher temperature cure, the performance properties can be equal to or greater than the properties observed with curing only at 22 °C curing. The results in this report indicate that in order to meaningfully measure and report the performance properties of Saltstone, one has to know the time/temperature profile conditions under which the Saltstone will be cured. This will require thermal modeling and actual time/temperature profiles within the vaults under various pour schedules to determine (1) an average profile of time and temperature under normal processing conditions and (2) a conservative (worst case) time/temperature profile. Samples can then be cast and cured in the laboratory under these time and temperature profiles prior to measurement of the performance properties of the product waste forms

From a processing perspective, a higher initial curing temperature decreased the set time to 1 day at both 40 °C and 60 °C and eliminated any bleed volume that was present for those samples that exhibited bleed at room temperature. However, the bleed water return system in the Saltstone Disposal Facility may remove bleed water before it can be reabsorbed.

Aluminate concentrations at levels greater than 0.20 M in these salt solutions can lead to positive or negative effects on the performance properties. At a curing temperature of 22 °C, aluminate increases Young's modulus and the compressive strength while reducing the total porosity. This generally corresponds to an improved (decreased) permeability (hydraulic conductivity) for Saltstone which is a positive outcome. On the other hand, with increased aluminate concentration there is a significant increase in heat of hydration that may limit pour schedule and must be considered in estimating the time/temperature profile to which Saltstone will be subjected during curing as discussed above. That is, higher temperatures in the vault (due to the higher heats of hydration) may present a greater challenge in controlling the curing time and temperature profile to achieve the desired performance properties.

The results of this study demonstrate that decreasing the w/cm ratio or increasing the slag content of the premix increases the performance properties of Saltstone. Predictive models were generated for these higher aluminate Salt Waste Processing Facility (SWPF) mixes that identify the important parameters that control Young's modulus, porosity and heat of hydration. These parameters include w/cm ratio, slag content, temperature, and aluminate, nitrate, nitrite and free hydroxide concentrations in the salt solutions. These models and data sets will serve as the basis to which new data from future batches can be added that in turn allow for a revision to the models with the expanded parameter ranges.

The heat of hydration measurements for these mixes demonstrated that aluminate and higher slag content (at the expense of fly ash) increase the total heat output and result in projected adiabatic temperature increases between 70 °C to 85 °C. The actual temperature increase in the vaults will be less than this due to heat losses which can be predicted by thermal modeling.

TABLE OF CONTENTS

LIST OF FIGURES

LIST OF TABLES

LIST OF ACRONYMS

ACTL	Aiken County Technology Laboratory
CBO	Carbon Burn-Out
CSH	Calcium Silicate Hydrate
E	Young's Modulus
FA	Class F Fly Ash
BFS	Blast Furnace Slag
DSS	Decontaminated Salt Solution
GVS	Grout Variability Study
OPC	Ordinary Portland Cement
PA	Performance Assessment
SDF	Saltstone Disposal Facility
SPF	Saltstone Production Facility
SRNL	Savannah River National Laboratory
SRNS	Savannah River Nuclear Solutions
SRS	Savannah River Site
SWPF	Salt Waste Processing Facility
TR	Trial Run
w/cm	Water to Cementitious Material Ratio

1.0 INTRODUCTION

At the Saltstone Production Facility (SPF), decontaminated salt solution (DSS) is combined with premix (a mixture of portland cement (OPC), blast furnace slag (BFS) and Class F fly ash (FA)) in a Readco mixer to produce fresh (uncured) Saltstone. After transfer to the Saltstone Disposal Facility (SDF) the hydration reactions initiated during the contact of the premix and salt solution continue during the curing period to produce the hardened waste form product. The amount of heat generated from hydration depends on the composition of the decontaminated salt solution being dispositioned as well as the grout formulation. Preliminary studies revealed that increased levels of aluminate in the feed cause a significant increase in the heat generation [1]. The additional aluminate projected for SWPF mixes results from the caustic treatment of High- Level waste sludge to remove some of the aluminum prior to vitrification. This dissolved aluminate from the sludge is then added to the SWPF salt batches that will be treated at the Saltstone Production Facility.

This report details the results from Task 2 of the Saltstone Variability Study for FY09 which was performed to determine the impact of higher aluminate concentration in the DSS on the processing and performance properties of Saltstone [2, 3]. Two separate campaigns, designated Phase 8 and Phase 9, were carried out under Task 2. Statistical analyses and designs were used to search for correlation between properties and to develop linear models to predict property values based on parameters such as w/cm ratio, slag content, and chemical constituents of the salt solution.

Due to the higher heats of hydration for mixes containing higher levels of aluminate and the resultant higher temperatures in the SDF under normal pour schedules, the properties of the Saltstone mixes were measured as a function of temperature and time of curing. The temperature of curing ranged mainly from 22°C to 60 °C although one sample was cured at 75 °C. Results of this study demonstrated that time, temperature and the sequence of curing had significant effects on the performance properties of Saltstone. Therefore, this report in addition to presenting the results on the impact of aluminate on Saltstone properties also focuses significantly on the impact of curing conditions of time and temperature on Saltstone properties.

2.0 EXPERIMENTAL

2.1 Materials

The cementitious materials were obtained from Saltstone in five gallon containers and are listed in Table 2-1. These materials were specified in a contract for Saltstone cementitious materials and arrived with the delivery of the cementitious materials to Saltstone. The materials were transferred to smaller high-density polyethylene bottles at Aiken County Technology Laboratory (ACTL) and tightly sealed. Maintaining these materials in a tightly sealed container limits the exposure of the materials to humid air and hydration of the materials prior to use. Table 2-1 also contains the wt% contribution of each material used to make the premix. The fly ash used in this study was a material that had been thermally treated by the Vendor to remove most of the carbon and ammonia (carbon burnout or CBO fly ash).

Table 2-1 Saltstone Cementitious Materials and Current Premix Blend

Material	Category	Vendor	Premix Blend (wt%)
Portland cement (OPC)	Type II	Holcim	10
Blast Furnace slag (GGBFS)	Grade I or II	Holcim	45
Fly ash (FA)	Class F	SEFA	45

2.2 Experimental Design

The mixes prepared for this study were included in either Phase 8 or 9 of the Saltstone Variability study. Phase 8 mixes were batched following the design presented in Table 2-2. The rows highlighted in blue were replicate runs of the central point of the design. The salt solutions simulated in Phase 8 (and Phase 9) are based on projections of the SWPF DSS with variation as noted in Table 2-2.

Table 2-2 Design for Phase 8 of the Saltstone Variability Study

	SWPF Grout Variability Study Phase 8 Aluminate As Batched								
Run Number	Simulant	Temp	Water/Premix	Slag	Added OH	Free OH	Nitrate plus Nitrite	Phosphate	Aluminate
Run Order	Number	°C	Ratio	Wt %	Molarity	Molarity	Molarity	Molarity	Molarity
GVS87	1	22	0.55	52.5	3.54	2.41	2.800	0.0073	0.2816
GVS88	2	22	0.60	45	2.37	1.91	3.300	0.0073	0.1144
GVS89	3	22	0.50	45	3.37	2.91	3.300	0.0073	0.1144
GVS90	4	22	0.60	60	3.37	2.91	2.300	0.0073	0.1144
GVS91	5	22	0.50	45	4.71	2.91	2.300	0.0073	0.4488
GVS92	6	22	0.50	60	2.37	1.91	2.300	0.0073	0.1144
GVS93	7	22	0.60	60	4.71	2.91	3.300	0.0073	0.4488
GVS94	8	22	0.60	45	3.71	1.91	2.300	0.0073	0.4488
GVS95	9	22	0.50	60	3.71	1.91	3.300	0.0073	0.4488
GVS96	10	22	0.55	52.5	3.54	2.41	2.800	0.0073	0.2816

The design for Phase 9 is provided in Table 2-3. This design uses a single simulant with 0.28 M aluminate and basically varies the w/cm ratio over the range of 0.50 to 0.65 in 0.05 increments

for 2 levels of slag content (45 wt % and 60 wt %). GVS 97 and GVS 106 were mixes batched with higher OPC content at the expense of the CBO FA.

Table 2-3 Design for Phase 9 of the Saltstone Variability Study

	SWPF Grout Variability Study Phase 9 Aluminate									
Run Number	Temp	Water/Premix	OPC	FA	Slag	Added OH	Free OH	Nitrate plus Nitrite	Phosphate	Aluminate
Run Order	°C	Ratio	Wt %	Wt %	Wt %	Molarity	Molarity	Molarity	Molarity	Molarity
GVS97	22	0.575	15	40	45	3.54	2.41	2.457	0.0073	0.2816
GVS98	22	0.50	10	45	45	3.54	2.41	2.457	0.0073	0.2816
GVS99	22	0.55	10	45	45	3.54	2.41	2.457	0.0073	0.2816
GVS100	22	0.60	10	45	45	3.54	2.41	2.457	0.0073	0.2816
GVS101	22	0.65	10	45	45	3.54	2.41	2.457	0.0073	0.2816
GVS102	22	0.50	10	30	60	3.54	2.41	2.457	0.0073	0.2816
GVS103	22	0.55	10	30	60	3.54	2.41	2.457	0.0073	0.2816
GVS104	22	0.60	10	30	60	3.54	2.41	2.457	0.0073	0.2816
GVS105	22	0.65	10	30	60	3.54	2.41	2.457	0.0073	0.2816
GVS106	22	0.575	20	35	45	3.54	2.41	2.457	0.0073	0.2816

2.3 Measurement of Properties

The measurements of heat of hydration [4], dynamic Young's modulus [5], porosity [6], and processing properties such as set time [7] were performed by the methods used previously. For compressive strength measurements, the samples were cast in 2 x 4 inch cylinders, capped, taped and then allowed to cure for 28 days prior to de-molding and measurement. Samples were made in triplicate for compressive strength and the results presented in this report are the average of the three measurements.

2.4 Curing at Different Temperatures

Samples were cured at ambient (also referred to as room temperature in this report) conditions in the laboratory (typically 22 °C), at 40 °C or at higher temperatures (52 °C or 60 °C). In all cases the cylinders in which the samples were cast, capped and securely taped. Measurement of the mass of the samples with container, lid and tape were made prior to and after curing to measure any mass loss during curing. At ambient temperature and at 40 °C curing conditions, essentially no change in the mass before and after curing was noted. For the 60 °C curing conditions, a mass loss on the order of 1 gram was noted. For reference, the Young's modulus cylinder and sample has a starting mass of ~ 1100 grams. Therefore, a loss of 1 gram corresponds to 0.1 wt % of the total mass of the sample.

The ovens have temperature gradients within the interior of the ovens. Therefore, the range of temperatures for a given sample may be as high as ± 5 °C about a set temperature. Thermocouples and thermometers were used to measure the actual temperatures within the oven. Figure 2-1 is a photograph of one of the ovens used in this study containing the samples being cured for Young's modulus and porosity measurements.

Figure 2-1 Photograph of one of the ovens used to cure the samples at elevated temperatures

3.0 RESULTS AND DISCUSSION

The results presented in this report were generated as part of Task 2 of the Saltstone Variability Study for FY09 (Phases 8 and 9) and focus on the impact of aluminate on the properties of Saltstone mixes. Phase 8 of this task used SWPF simulants with a baseline aluminate concentration equal to 0.28 M and a range of aluminate concentration from 0.11 M to 0.44 M. Phase 9 used an SWPF simulated salt solution containing 0.28 M aluminate for all the mixes and investigated the impact of w/cm ratio and slag content on the Saltstone properties. The results from Phase 8 mixes will be presented first to provide a reference baseline for contrast to the impact that higher aluminate concentrations have on the properties of Saltstone. Then, the results from Phase 9 mixes at 0.28 M aluminate are presented. Results on the correlation of performance properties using data from all the mixes are presented. Predictive property models were generated for these data sets and are also presented.

3.1 Phase 8 Mixes - Impact of Curing Temperature and Aluminate levels

Measurements of performance properties and indicators for the mixes batched as part of Phase 8 included compressive strength, Young's modulus, and total porosity. Values for these performance properties are presented below for 3 mixes (Table 3-1) selected to provide reference cases that help illustrate the impact of aluminate. The values for these performance properties at three curing temperatures are presented in Figures 3-1 and 3-2.

Table 3-1 Mix Designs of Three Mixes from Phase 8

Mix	w/cm	Aluminate	Nitrate	Slag	Fly Ash	Cement	Heat
		M	M	Wt %	Wt %	Wt %	J/g premix
GVS 88	0.60	0.11	2.72	45.0	45.0	10.0	174
TR 538	0.55	0.11	2.32	45.0	45.0	10.0	NM
GVS 96	0.55	0.28	2.32	52.5	37.5	10.0	235

GVS 88 is a mix that was batched using the currently projected baseline SWPF salt solution at 0.11 M aluminate with a w/cm ratio of 0.60 and the nominal 45:45:10 premix composition. The value for Young's modulus for GVS 88 is 7.3 GPa at 22 °C and the heat of hydration at 25°C was 174 J/g of premix. The impact of curing temperature on the performance properties of this mix is significant. For example, a decrease in both Young's modulus and compressive strength and an increase in total porosity were observed as the curing temperature was increased to 40 °C. However, when the curing temperature was increased to 60° C, the performance properties reversed this trend and began to improve as shown in Figure 3-1.

TR 538 is a mix similar to GVS 88 but batched with a w/cm ratio of 0.55. The Young's modulus and compressive strength values are slightly higher and the porosities lower for the GVS 88 mix relative to the TR 538 mix as expected for a mix with lower w/cm ratio. However, trends in the performance properties of TR 538 as a function of temperature are essentially the same as

observed for GVS 88. This turns out to be the general case for mixes containing salt solutions with low concentrations of aluminate (0.11 M).

In contrast, GVS 96 is a mix which typifies the dependence of performance properties on curing temperature for higher aluminate mixes. In this case the values of Young's modulus and compressive strength continually decrease while the total porosity continually increases throughout the curing temperature range covered. Figure 3-2 provides this data and can be contrasted to the same data for the mixes with lower aluminate levels (Figure 3-1).

The heat of hydration for mixes containing elevated levels of aluminate in the salt solution lead to increased heat of hydration. For example, the heat of hydration for mix GVS 96 is 235 J/g of premix at 28 days compared to 174 J/g of premix for GVS 88 (Table 3-1). Thus, at room temperature, the increased heat of hydration is reflective of additional hydration reactions which in turn lead to improvement in the performance properties of mixes cured under ambient conditions (22 °C).

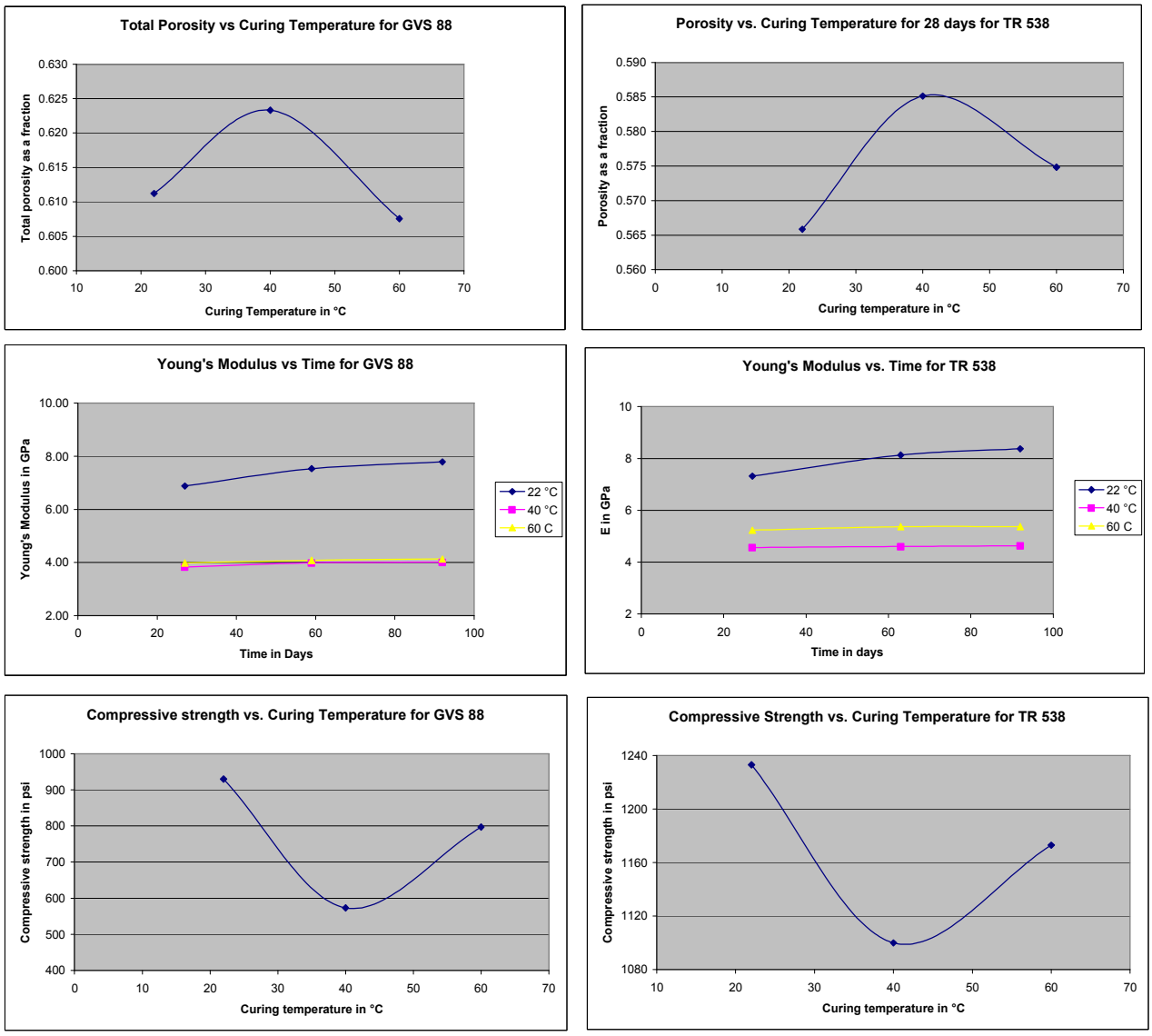

Figure 3-1 Performance properties of 2 mixes from Phase 8 with aluminate levels of 0.11 M as a function of curing temperature

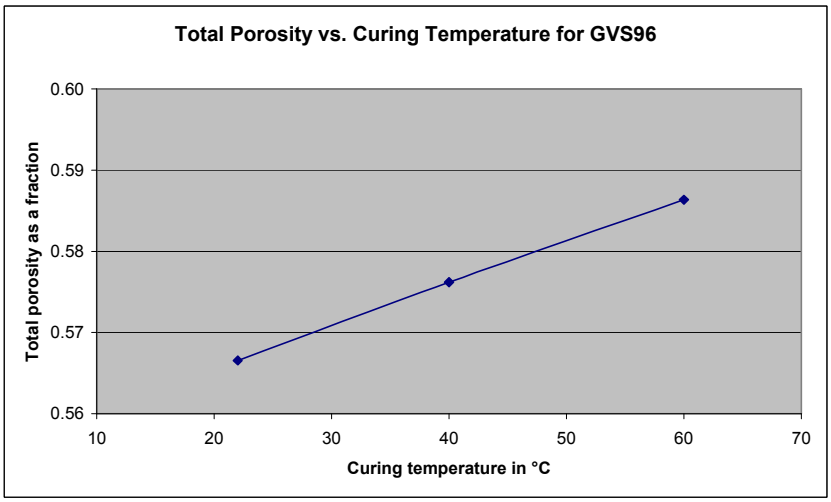

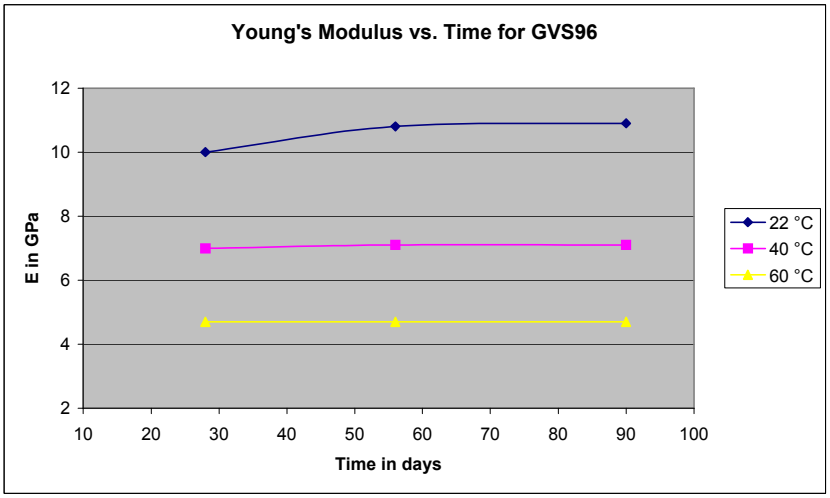

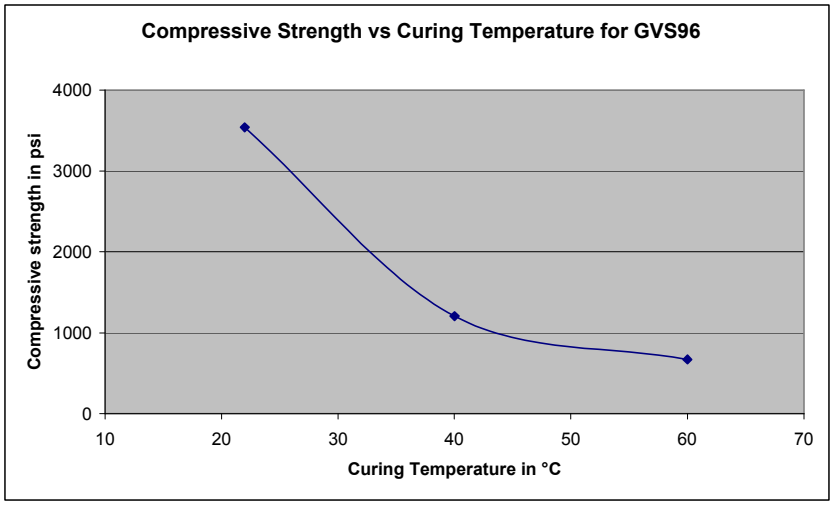

Figure 3-2 Performance properties of GVS 96, a mix with 0.28 M aluminate

3.2 Phase 9 – Young's Modulus as a Function of w/cm Ratio and Wt % Slag

The values of Young's moduli for the eight SWPF mixes (excluding the two mixes at higher portland cement levels which will be discussed separately below) for Phase 9 as a function of w/cm ratio at two different slag loadings are presented in Figure 3-3. In this case the samples were cured under sealed conditions at room temperature (22 °C). It is clear from this data that decreasing the w/cm ratio from 0.65 to 0.50 increases Young's modulus by ~ 25 % independent of the slag loading. Based on literature values of Young's modulus, this increase in E can be associated with order of magnitude changes in the permeability. For a reasonable reduction in w/cm ratio from the current nominal 0.60 to a reduced value of 0.55, the Young's modulus increased by ~ 8 %. The second conclusion that can be drawn from this data is that an increase in wt % slag from 45 to 60 wt % in the mix at the expense of fly ash increases Young's modulus by ~ 12 %. Therefore, by reducing the w/cm ratio and/or increasing the wt % slag content, an improvement in performance as measured by Young's modulus can be achieved for room temperature cured samples. As previously discussed, there is also an increase in Young's modulus for these samples as a result of an increase in the aluminate level from 0.11 M in the current baseline to 0.28 M in the baseline with added aluminate.

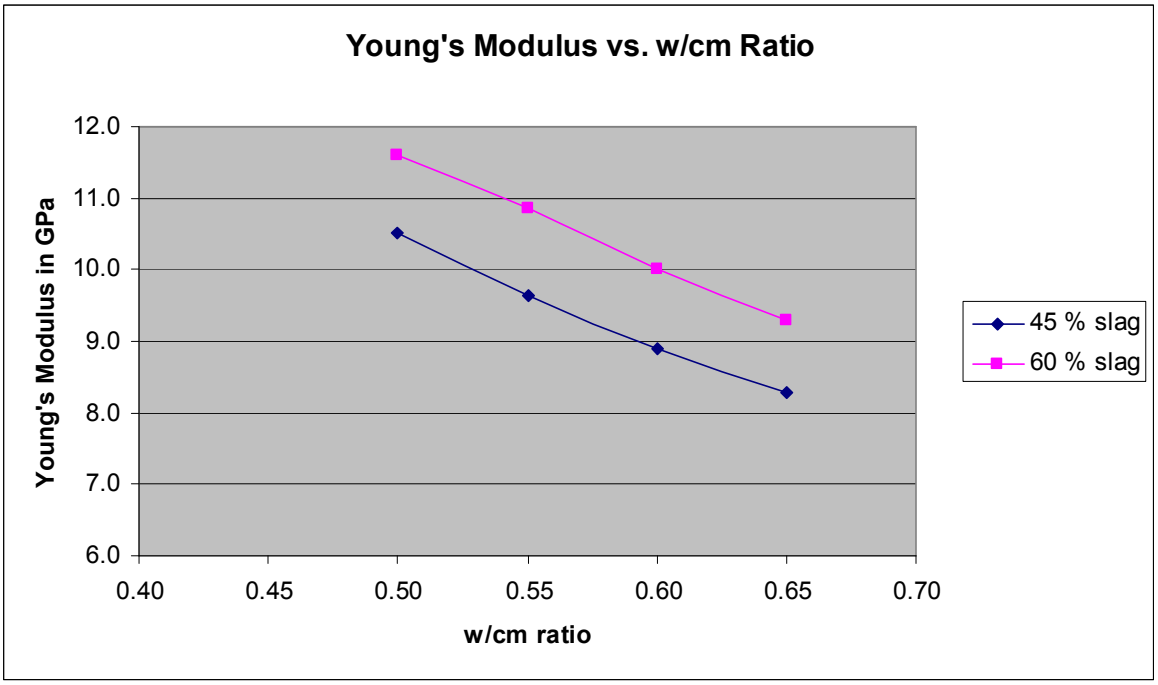

Figure 3-3 Young's modulus (E) values for eight SWPF mixes as a function of w/cm ratio and wt % slag for samples cured at 22 °C

Samples of these mixes were also cured in sealed cylinders in ovens at 40 °C and 60 °C for 28 days to determine the impact of curing temperature on the performance properties of Saltstone. One additional sample was cured at 60 °C for 1 week, removed from the oven and then cured for

the remaining 21 days at ambient temperature. The values for the 28 day Young's modulus for each of these samples are provided in Figures 3-4 and 3-5.

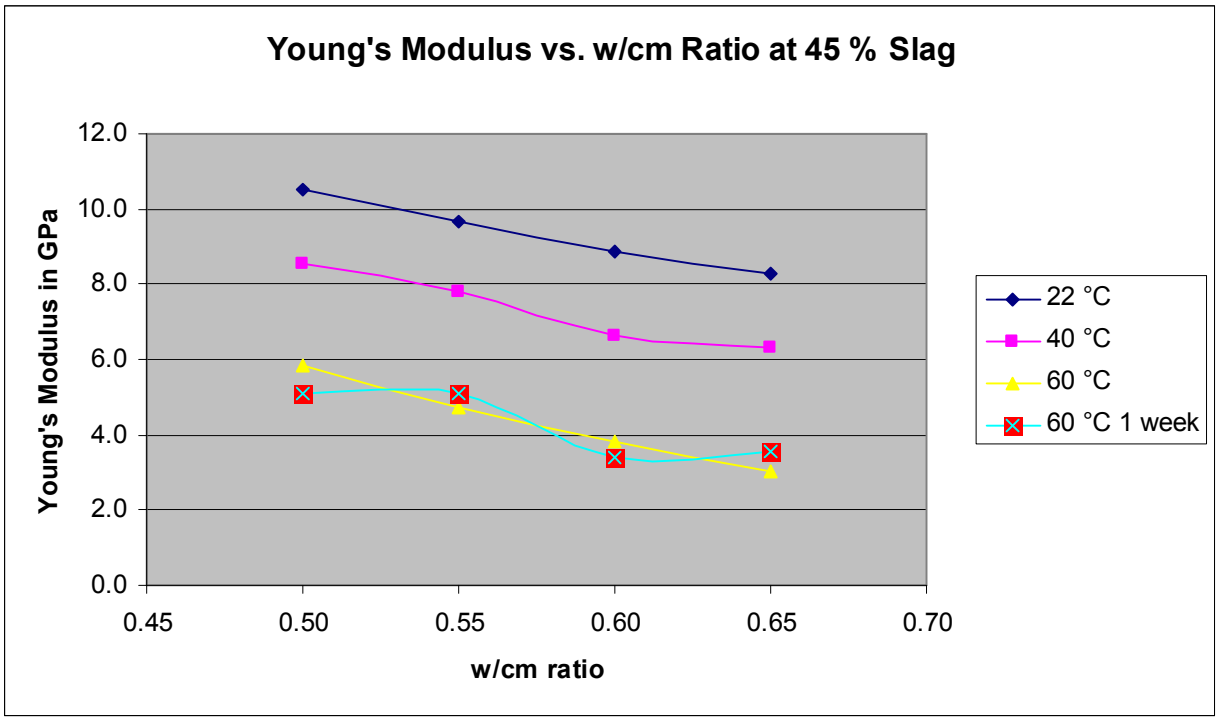

Figure 3-4 Young's modulus values for 4 SWPF mixes containing 45 wt % slag after curing at the indicated temperatures for 28 days. The data points for the red squares were obtained on the samples removed from the 60 °C oven at 1 week and measured at 28 days.

Figure 3-4 reveals that E values are significantly reduced at higher curing temperatures. In fact, E is reduced by approximately 60 % for samples cured at 60 °C compared to 22 °C. Furthermore, the E values for the samples initially cured at 60 °C for one week and then removed and cured at ambient temperature are essentially identical to the samples cured for the entire 28 days at 60 °C. This implies that the hydration reactions are complete by the end of one week at a 60 °C curing temperature.

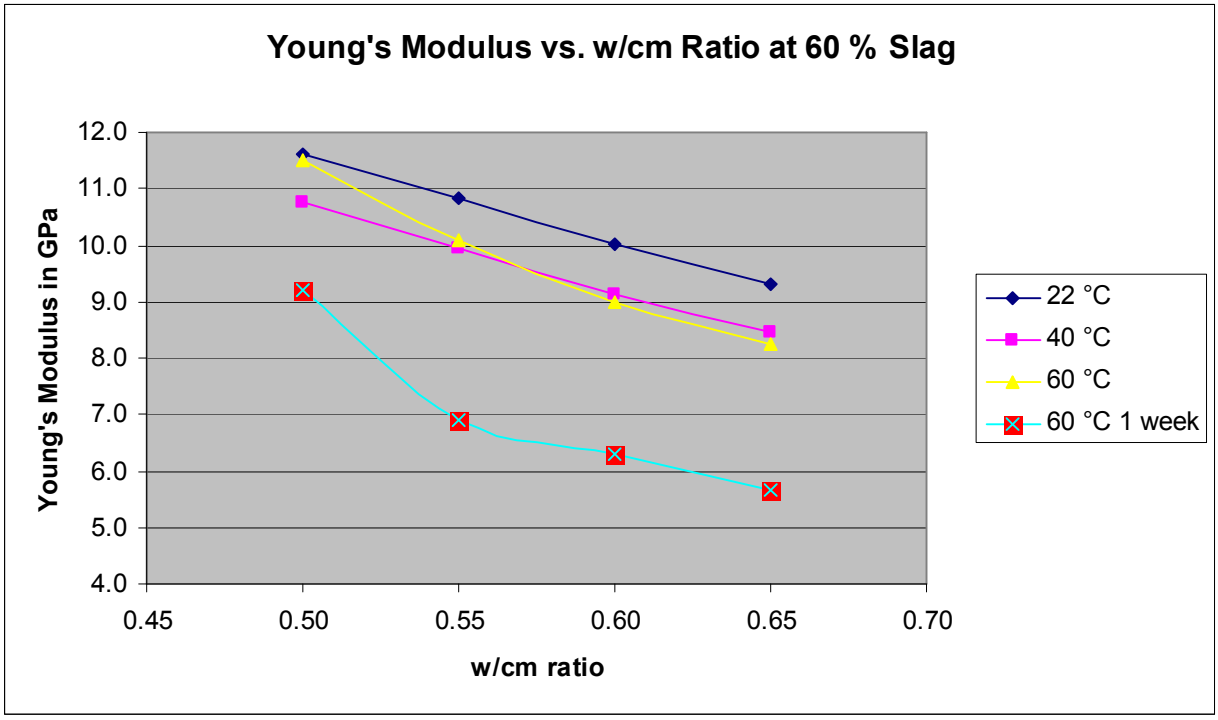

Figure 3-5 Young's modulus values for 4 SWPF mixes containing 60 wt % slag after curing at the indicated temperatures for 28 days The data points for the red squares were obtained on the samples removed from the 60 °C oven at 1 week and measured at 28 days.

Figure 3-5 shows that the reduction in E at higher curing temperatures for mixes batched with a slag content of 60 wt %. Although the reduction in E is still evident, it is much reduced relative to the mixes with 45 wt % slag (Figure 3-4). This reduction in E in the case of the 60 wt % slag mixes is only 10 % on average over the range of temperatures used for curing compared to the 60 % reduction for the 45 wt % slag mixes. This demonstrates that the impact of curing temperature on E values may be mitigated by increasing the slag content of the mix.

In the 60 wt % slag mix, removal of the samples from the 60 °C oven at 1 week revealed a marked decrease in E values relative to the E values for the samples cured at 60 °C for 28 days. In the 45 wt % slag mixes, the E values were the same for both cases. This implies that in addition to the curing temperature, the length of time at curing temperatures is also important.

Two mixes were batched in Phase 9 with 15 and 20 wt % portland cement, an increase that took place at the expense of fly ash content. Only two mixes were prepared with higher cement levels based on the limited number of samples that can be managed in one phase. These results demonstrated that the mix batched with 20 wt % portland cement actually has a higher E value at a 60 °C curing temperature for 28 days than does the same mix cured at 22 °C. However, the samples cured at 60 °C for 1 week had a reduced value of E consistent with other mixes (see Section 3.3). This data suggests that an increased level of portland cement (much like increased levels of slag) may also help mitigate the reduction in performance properties observed for mixes cured at higher temperatures.

Table 3-2 Young's Modulus Values (E in GPa) for Mixes containing 15 and 20 Wt % Slag as a Function of Curing Time and Temperature

Mix #	OPC Content	Curing Time	22°C	40°C	60°C	60°C
	Wt %	days				1 week
GVS 97	15	28	9.5	8.0	5.1	4.3
GVS 106	20	28	9.1	7.8	9.8	7.8

3.3 Young's Modulus as a Function of Time, Temperature and Sequencing

As presented earlier, one additional sample from each of the mixes GVS98 through GVS105 of Phase 9 was cured in sealed containers at 60 °C for 1 week, removed from the mold and then placed in sealed plastic bags for continued curing at ambient conditions over the 28 days period of this test. Measurements of Young's modulus for these samples were performed at 7, 14, and 28 and 70 days (see Figure 3-6). The top four curves were results from samples that contained 60 wt % slag and were in the order starting from the top curve (GVS 102) of 0.50 to 0.65 w/cm ratio (GVS 105). These mixes continue to hydrate with time as evidenced by the slightly higher E values at 70 days. The bottom four curves are results from samples that contained 45 wt % slag and are in the order starting from the GVS98 curve and continuing lower in E values as the w/cm ratio increased from 0.50 to 0.65 w/cm (GVS 101). These samples show essentially no improvement in E as a function of time (no signal could be obtained for GVS 101 at 70 days).

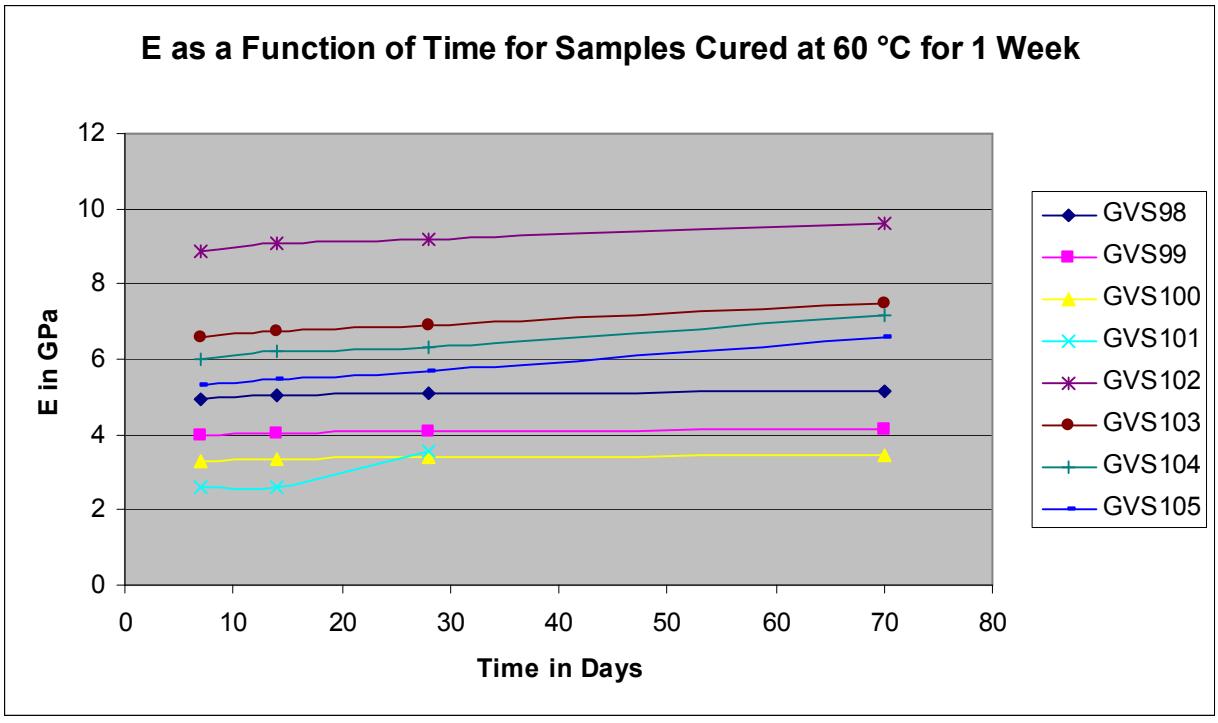

Figure 3-6 Time dependence of E in GPa for Phase 9 mixes subjected to an initial cure temperature of 60 °C for 1 week followed by a final cure at 22 °C

These results demonstrate that final performance of the grout is influenced by curing temperature and time. In order to better understand this relationship, time dependent testing was conducted to determine this impact on performance properties. In addition, the sequencing of the curing conditions was also investigated. This was accomplished by curing first at high temperatures followed by a room temperature cure versus curing first at room temperature followed by curing at higher temperatures.

The first set of tests followed the sequence of curing at 60 °C for either 1, 2 or 4 days followed by additional curing up to 28 days at room temperature. Figure 3-7 presents Young's modulus data obtained for samples batched to the formulation of GVS 103 (0.55 w/cm ratio and 60 wt % slag) as a function of time of curing at 60 °C. The three samples were removed from the 60 °C oven at 1, 2 and 4 days and then Young's modulus was measured for each sample at a frequency shown in the Figure 3-7. The time dependence in Figure 3-7 reveals that samples subjected to an initial cure time as short as one day at 60 °C do not reach values of E obtained for ambient temperature curing. If the initial cure at 60 °C was maintained for 4 days, no further improvement in E was observed.

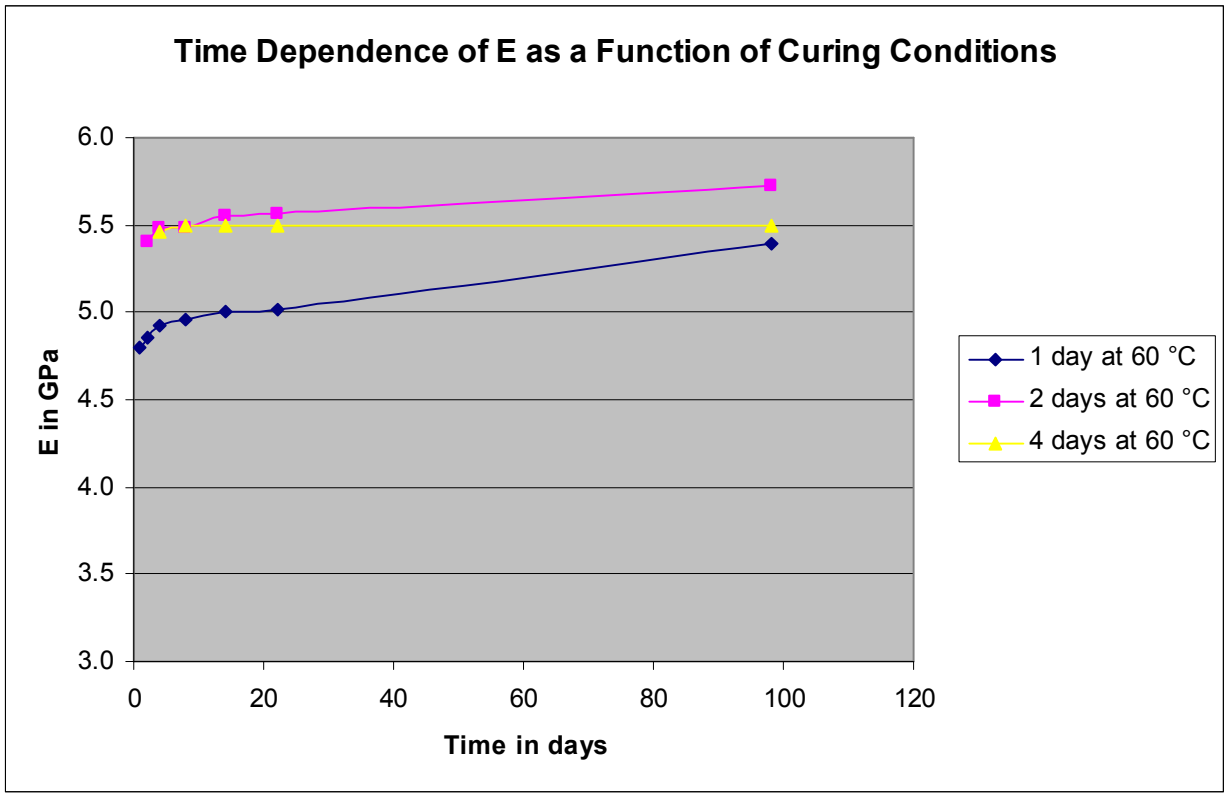

Figure 3-7 Time dependence of E in GPa for GVS 103 (60 wt % slag) at indicated time and temperature profiles

The second set of tests followed the sequence of curing at 22 °C for 1, 2, 3 or 4 days followed by additional curing up to a total of 7 days from batching at 52 °C. The samples were then removed

from the oven and cured over the remaining 28 days at room temperature. These results reveal that samples of Saltstone subjected to an initial curing at ambient condition and then subjected to a relatively short curing period at 60 °C had Young's moduli values equal to or higher than an equivalent samples cured only at room temperature. The results are summarized in Figure 3-8.

Two additional samples were tested and the results are also included in Figure 3-8. One of the samples was cured only at 22 °C while the other was cured for 7 days at 60 °C and then removed and placed at room temperature. Consistent with the results already presented, the initial 7 day cure at higher temperature leads to a lower value of Young's modulus which does not improve much with time. The sample kept at 22 °C at all times, shows a steady increase in value with curing time.

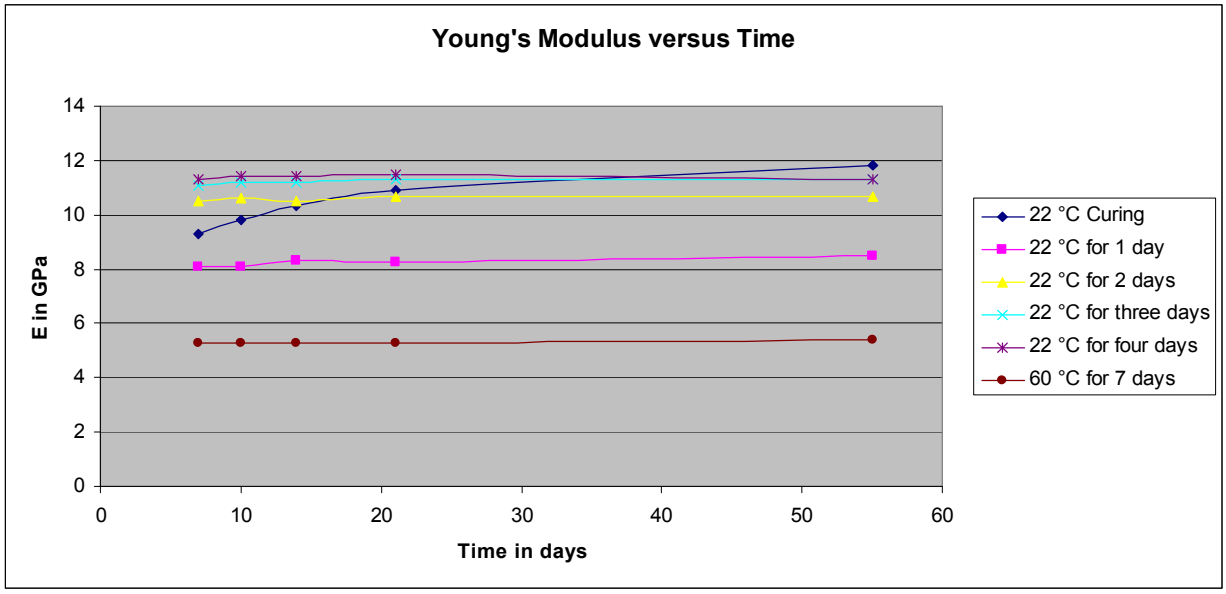

Figure 3-8 Time dependence of E in GPa for GVS 103 (0.55 w/cm ratio and 60 wt % slag) at indicated time and temperature profiles

Figure 3-9 provides the equivalent data for GVS 99 mixes (45 wt % slag) versus under the same sequences shown in Figures 3-8 and 3-9. The same trends are observed in both cases and demonstrate that this lack of symmetry in development of E with curing sequence is also observed at the nominal premix composition.

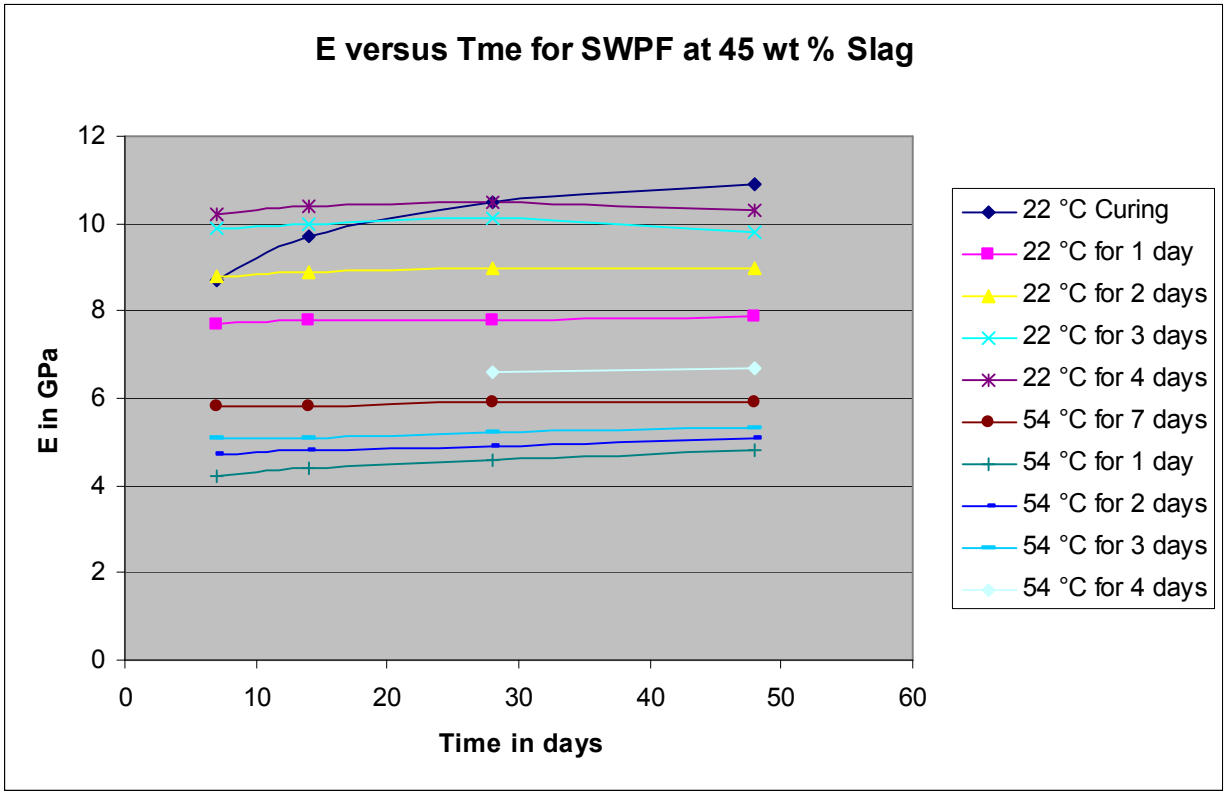

Figure 3-9 Time dependence of E in GPa for GVS 99 (0.55 w/cm ratio and 45 wt % slag) at indicated time and temperature profiles

These results can be explained in general by assuming that structure of the calcium silicate hydrate (CSH) gel formed initially with a 22 °C curing temperature is different than the structure of the CSH gel formed at higher temperatures [8]. The CSH gel at room temperature can continue to hydrate and strengthen at both room temperature and higher curing temperatures. On the other hand, the CSH gel formed at higher temperatures is resistant to further hydration at any temperature. For example, the outer layer of the CSH particles formed at higher temperatures may have low solubility and diffusivity and therefore preclude the dissolution and diffusion necessary for additional hydration reactions to occur. Further characterization of the microstructures of Saltstone cured under different temperatures is required to confirm this assumption.

3.4 Dynamic Young's Modulus for GVS 103 Cured at 75 °C

One sample from GVS 103 was cured in an oven at 75 °C of 8 days followed by an additional 19 days at room temperature. This sample had a maximum value for E of only 4.5 GPa compared to a value of 11 GPa after 28 days for a sample cured at room temperature. Therefore, the trend of reduced values of E as the temperature of curing is increased is still maintained up to a temperature of 75 °C. This E value of 4.5 GPa reached at 8 days (time of the first measurement) did not improve with additional time of curing at room temperature.

3.5 Porosities as a Function of Curing Temperature and Time

The impact of w/cm ratio and slag content on total porosity were determined for the Phase 9 SWPF mixes at 0.50, 0.55, 0.60, and 0.65 w/cm ratios for premixes containing either 45 or 60 wt % slag. The total porosity values (expressed as fractions) for samples cured at 22 °C are shown in Figure 3-10. The total porosity decreases with (1) decreasing w/cm ratio and (2) increasing slag content. This is consistent (porosity and E are inversely related) with the trend of Young's Modulus values for these same mixes as shown in Figure 3-2.

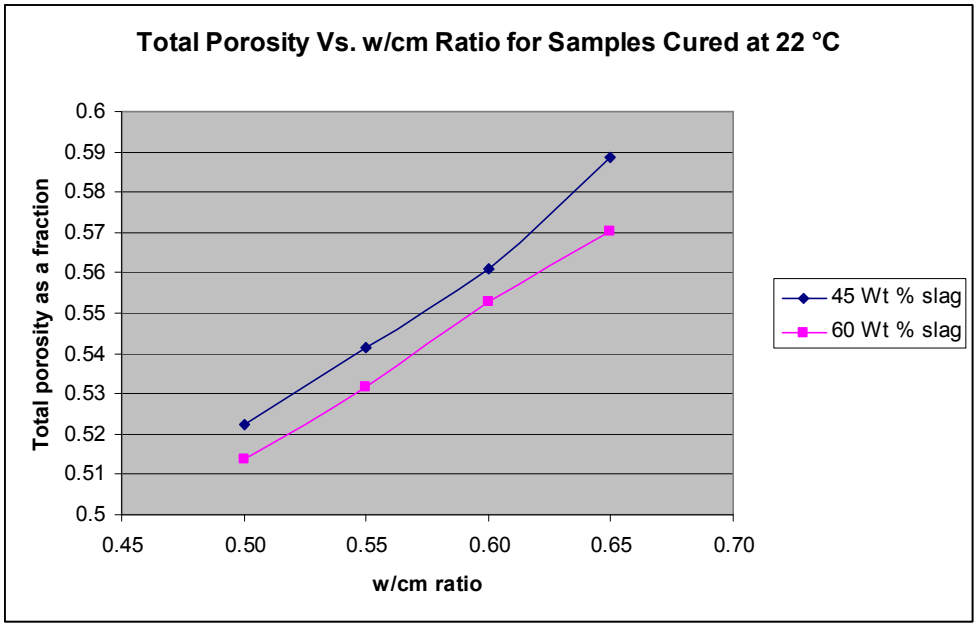

Figure 3-10 Total porosity for mixes batched with either 45 or 60 wt % slag as a function of w/cm ratio. Porosities were measured after 28 days of curing at 22 °C.

Figure 3-11 shows the dependence of total porosity on curing temperature for samples that contain 45 wt % slag in the premix. The total porosity increases with increasing curing temperature which again, in the expected inverse relationship between E and porosity, corresponds to the data obtained for Young's modulus over these variables (Figure 3-2).

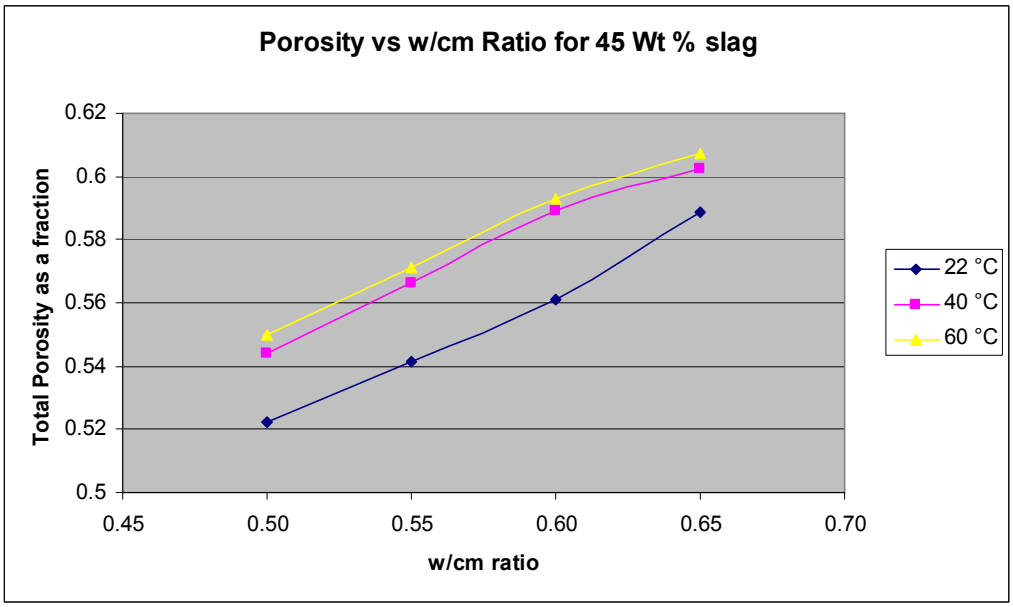

Figure 3-11 Total porosity as a function of w/cm ratio for 3 cure temperatures

Figure 3-12 shows the dependence of total porosity on curing temperature for samples that have 60 wt % slag. The total porosity increases with increasing curing temperature and corresponds to the data obtained for Young's modulus over these variables (Figure 3-3).

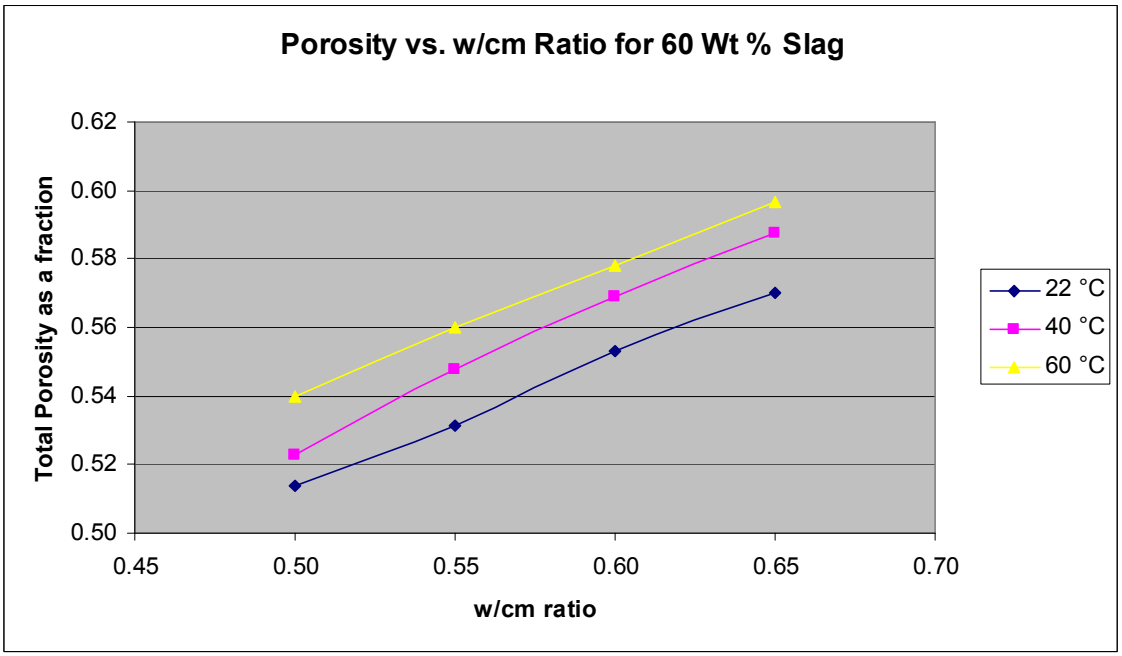

Figure 3-12 Total porosity as a function of w/cm ratio for three curing temperatures and 60 wt % slag

3.6 Heat of Hydration

The heat of hydration data for Phase 9 mixes are provided in Table 3-4. As the w/cm ratio increases for both the 45 and 60 wt % slag mixes, the heat of hydration normalized to the premix content actually increases. This is most likely due to the facts that (1) there is a better dispersion of the cementitious particles in grouts with higher water content and (2) there is more water available for hydration at higher water content. However, the heat of hydration, normalized to the mass of grout is essentially the same for the set of four mixes with 45 wt % slag at 125 J/g and for the same set of four mixes with 60 wt % slag at 151 J/g. The difference in heat generation between these two sets is mainly due to the differences in slag content. However, the model produced and discussed in Section 3.7 of this report details the dependence of heat of hydration on all significant parameters for the combined 8 and 9 phases.

Table 3-3 Heat of Hydration and Final Temperature Increase for Phase 9 Mixes

Identifier	Heat of Hydration	Peak time	Heat of Hydration	Cp	Temp Rise	Initial Temp	Final Temp
	J/g of cm	hours	J/g of grout	J/g/°C	°C	°C	°C
GVS98	210	54	124	1.77	69.8	25.0	96.3
GVS99	220	54	124	1.93	64.6	25.0	91.1
GVS100	230	58	125	1.81	69.1	25.0	95.6
GVS101	239	51	125	1.97	63.8	25.0	90.3
GVS102	256	27	149	1.77	84.4	25.0	110.9
GVS103	270	30	153	1.80	84.6	25.0	111.1
GVS104	277	33	151	1.88	80.1	25.0	106.6
GVS105	286	35	150	1.90	79.0	25.0	105.5

The heat capacities for each mix were measured and provided in the Table 3-3. From this data, one can calculate the temperature increase that would be predicted if the system were maintained adiabatically. The final calculated adiabatic temperature rise is then the sum of the temperature rise due to the heat of hydration and the initial solution temperature increase observed in the first minutes of mixing of ~ 1.5 °C. The initial increase in temperature is measured upon mixing the premix with the salt solution and consequently is not captured during isothermal calorimetry. The adiabatic temperature increases are significantly higher than the corresponding temperature increases calculated for mixes at lower aluminate levels (~0.1 M).

3.7 Processing Properties

Task 2 focused mainly on the performance properties of the Saltstone mixes. However, the processing properties must also be acceptable for processing at SPF. The processing property results for Phase 9 mixes are presented in Table 3-4. Two of the mixes had gel times less than 20 minutes and the yield stress and plastic viscosity were relatively high for some of the mixes. Acceptance criteria for the flow properties have yet to be established and pumping calculations will be required to determine these criteria. At both 40 °C and 60 °C curing temperatures, there was no bleed and the set times, which were either 2 or 3 days at 22 °C, were all reduced to less than 1 day.

Table 3-4 Processing Properties for Phase 9 Mixes

					Uncorrected		1 Day Bleed				Set Time		
Temp.	Identifier	Gel Time	Density	Flow	Yield Stress	Viscosity	22 °C	22 °C	40 °C	60 °C	22 °C	40 °C	60 °C
°C		minutes	g/mL	cm	Pa	cP	Vol %	Vol %	Vol %	Vol %	Days	Days	Days
22	GVS97	20	1.742	21.0	4.6	123.7	0.5	0.5	0.0	0.0	2	1	1
22	GVS98	20	1.773	18.5	7.9	202.9	0.0	0.0	0.0	0.0	2	1	1
22	GVS99	30	1.760	20.5	5.0	127.7	0.5	0.5	0.0	0.0	3	1	1
22	GVS100	40	1.709	22.5	3.6	94.8	0.6	0.6	0.0	0.0	3	1	1
22	GVS101	40	1.709	25.8	2.2	52.9	0.5	0.5	0.0	0.0	3	1	1
22	GVS102	10	1.839	18.5	10.5	181.6	0.0	0.0	0.0	0.0	2	1	1
22	GVS103	20	1.768	20.8	6.6	118.2	0.0	0.0	0.0	0.0	2	1	1
22	GVS104	20	1.737	23.5	4.6	78.6	0.3	0.3	0.0	0.0	2	1	1
22	GVS105	20	1.714	24.9	3.3	57.8	0.3	0.3	0.0	0.0	2	1	1
22	GVS106	10	1.744	21.3	5.6	108.1	0.0	0.0	0.0	0.0	2	1	1

The processing properties for the Phase 8 mixes are shown in Table 3-5.

Table 3-5 Processing Properties for Phase 8 Mixes

					Uncorrected		1 Day Bleed				Set Time		
Temp.	Identifier	Gel Time	Density	Flow	Yield Stress	Viscosity	22 °C	22 °C	40 °C	60 °C	22 °C	40 °C	60 °C
°C		minutes	g/mL	cm	Pa	cP	Vol %	Vol %	Vol %	Vol %	Days	Days	Days
22	GVS87	30	1.761	22.00	4.2	111.5	0.7	0.6	0.0	0.0	3	1	1
22	GVS88	> 70	1.716	24.40	3.0	71.9	2.4	2.6	0.0	0.0	1	1	1
22	GVS89	40	1.788	19.00	6.6	185.9	0.0	0.0	0.0	0.0	1	1	1
22	GVS90	50	1.743	22.00	5.7	95.3	0.0	0.0	0.0	0.0	1	1	1
22	GVS91	20	1.783	18.70	6.6	193.9	0.0	0.0	0.0	0.0	2	1	1
22	GVS92	20	1.842	16.70	15.8	215.7	0.0	0.0	0.0	0.0	1	1	1
22	GVS93	30	1.756	23.80	3.4	86.4	0.0	0.0	0.0	0.0	2	1	1
22	GVS94	30	1.709	24.80	3.4	71.0	0.7	0.7	0.2	0.0	3	1	1
22	GVS95	20	1.800	19.50	7.7	161.0	0.0	0.0	0.0	0.0	3	1	1
22	GVS96	30	1.770	21.50	5.2	111.0	0.2	0.2	0.0	0.0	3	1	1

3.8 Correlations

One of the goals of this work was to determine the correlation between Young's modulus and permeability. Initial efforts to determine the feasibility of this approach are in progress for FY09 and will be reported separately. It is anticipated that permeability will be related to total porosity and/or pore size distribution [9]. Therefore, a correlation of Young's modulus with total porosity would provide an important connection to and validation of the goal. The data obtained in this report have been compiled with the previous data sets to generate an overall plot of Young's modulus versus porosity as provided in Figure 3-13. The center red line is the linear fit with an R^2 value of 80.0%. The equation is:

$$\text{Young's modulus} = 38.62 - 0.54 * \text{Porosity}$$

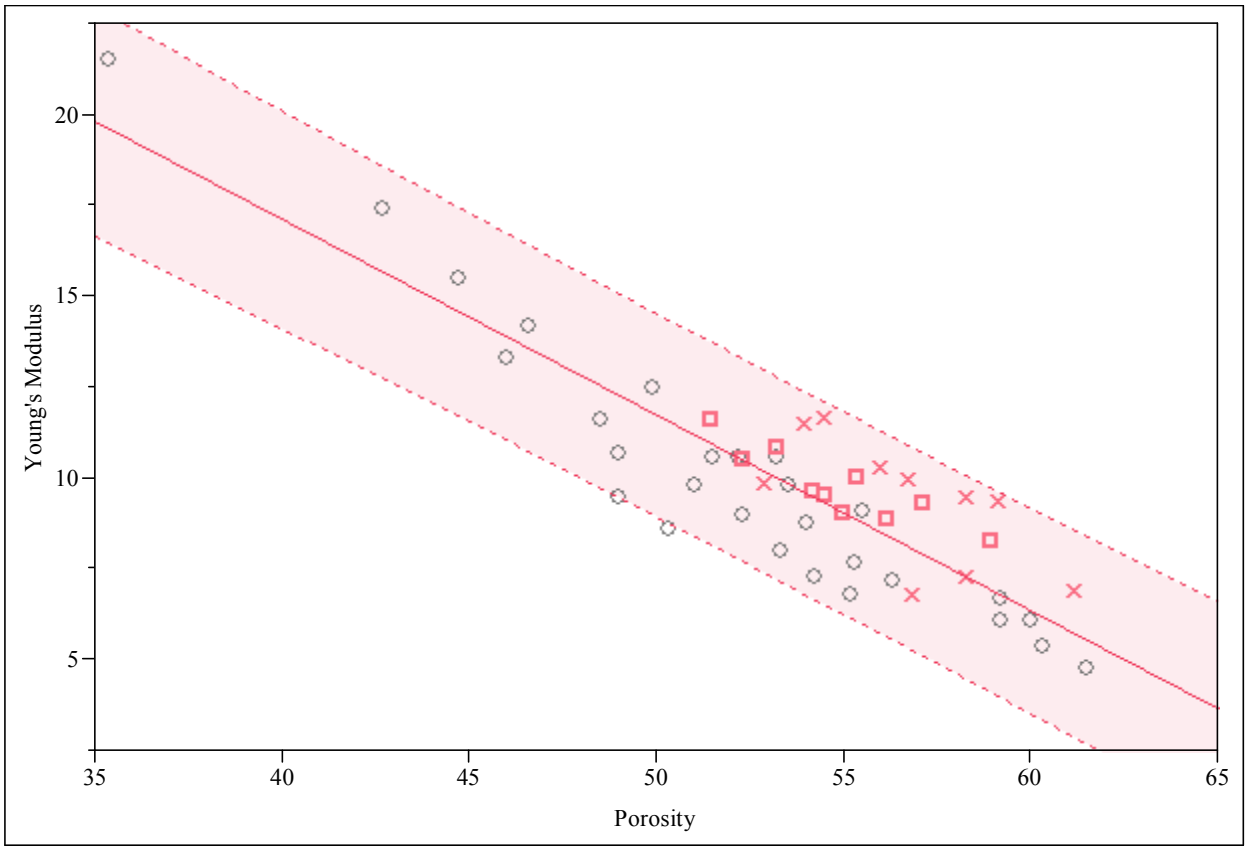

Figure 3-13 Bivariate fit of Young's modulus and total porosity for mixes of Phases 8 and 9 measured at 22 °C. The red "x' represents phase 8 mixes and the red "square" represents phase 9 mixes while the black "circles" are from previous measurements of earlier phases of the variability study

The nature of the changes that occur as a function of curing temperature, time and sequence at the molecular level or the nano- and microstructural level to the calcium silicate hydrate phase is not known. In spite of this, the total porosity and Young's modulus values for Phases 8 and 9 at all curing temperatures (22, 40 and 60 °C) were introduced into the data set that generated Figure 3-13 to produce a new correlation with all of the data (Figure 3-14).

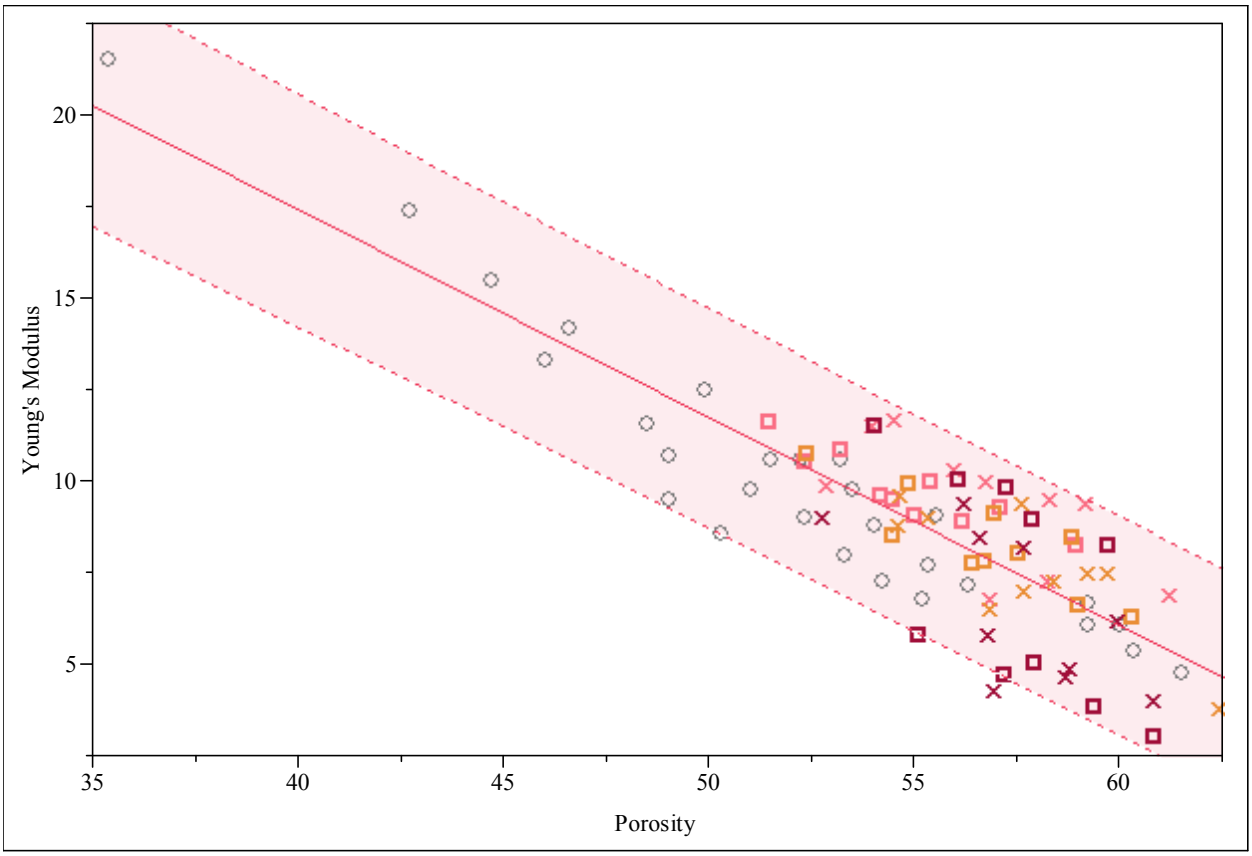

Figure 3-14 Bivariate fit of Young's modulus and total porosity for mixes of Phases 8 and 9 measured at all temperatures of curing. The legend for the data points is provided below

		Phase	Curing Temp
○	1		.
×	2	Phase 8	20
×	3	Phase 8	40
×	4	Phase 8	60
□	5	Phase 9	20
□	6	Phase 9	40
□	7	Phase 9	60

The center red line is the linear fit with an R^2 value of 74.0%. The equation is:

Young's modulus = 40.16 - 0.57*Porosity

There is structure visible within this overall plot indicating that some other factors may influence this correlation and as discussed above, may reflect different mechanisms in play at different curing temperatures. Future FY09 efforts with MCU and SWPF mixes will measure and integrate the values of Young's modulus and total porosity into this linear correlation.

3.9 Predictive Models

One of the goals of this work was to determine which parameters are important in determining the values of physical properties (responses) of the Saltstone mixes. In this Section of the report, the results of models for Young's modulus, total porosity and heat of hydration are presented.

For Young's modulus, the predicted versus actual values are plotted and provide a linear fit with an R^2 equal to 80 % (Figure 3-15). These data points are for Phases 8 and 9 and include mixes cured at all three temperatures.

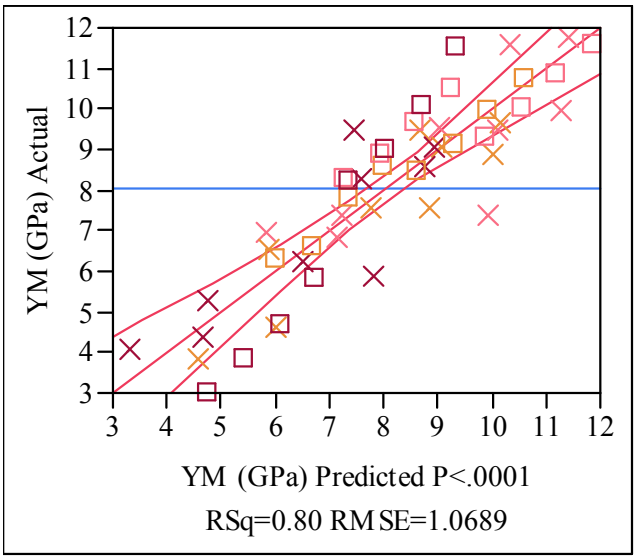

Figure 3-15 Actual versus predicted values of Young's modulus for samples of Phases 8 and 9 including results for samples cured at different temperatures

The model (equation) for prediction of E, where [ ] indicates Molarity and T is the temperature in °C, is:

E = 11.6 - 13.2•w/cm + 0.18•wt % slag + 5.00 [Aluminate] - 1.51• [Nitrate + Nitrite] - 0.06•T

For total porosity, the predicted versus actual values are plotted and provide a linear fit with an R^2 equal to 81 % (Figure 3-16). These data points are for Phases 8 and 9 and include mixes cured at all three temperatures.

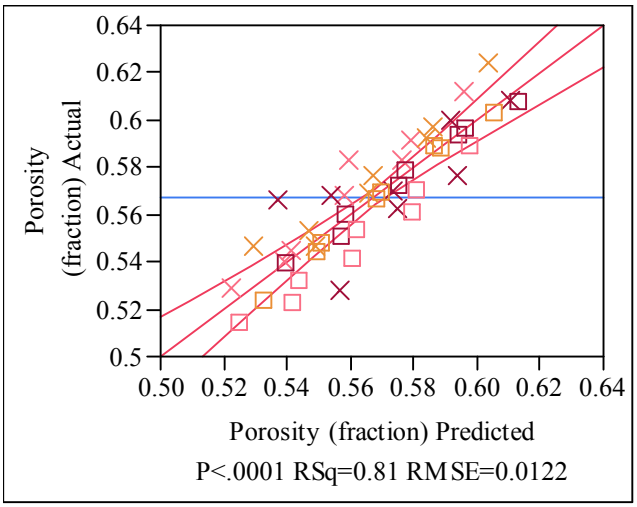

Figure 3-16 Actual vs. predicted values of total porosity for samples of Phases 8 and 9 and including different temperatures of curing

The model (equation) for prediction of total porosity (Φ) expressed as a fraction, where [ ] indicates Molarity and T is the temperature in °C, is:

$$\Phi = 0.35 + 0.37 \bullet w/cm - 0.001 \bullet wt\ \%\ slag + 0.019 \bullet [Nitrate + Nitrite] + 0.0004 \bullet T$$

Since Young's modulus and total porosity are inversely correlated, the coefficients in the models are of opposite sign for these two properties. Interestingly, aluminate concentration is not a statistically significant factor in the model for porosity but does play a role in the value of E.

So, for a change in w/cm ratio from 0.60 to 0.55, the models predict an increase in E of 0.7 GPa and a decrease in Φ of 0.019 (1.9 volume %). For a change in slag content (at the expense of fly ash) from the normal 45 wt % to 60 wt %, E increases by 2.7 GPa and Φ decreases by 0.015 (1.5 volume %). A change in Molarity of aluminate from 0.11 M to 0.28 M results in a predicted increase in E of 0.9 GPa. Both temperature of curing and the total nitrate plus nitrite concentrations give similar changes to E and Φ for a 40 °C change in temperature or a 1 molar change in nitrate plus nitrite concentration.

The heat of hydration in J/g of premix was also modeled and the results are provided in Figure 3-17.

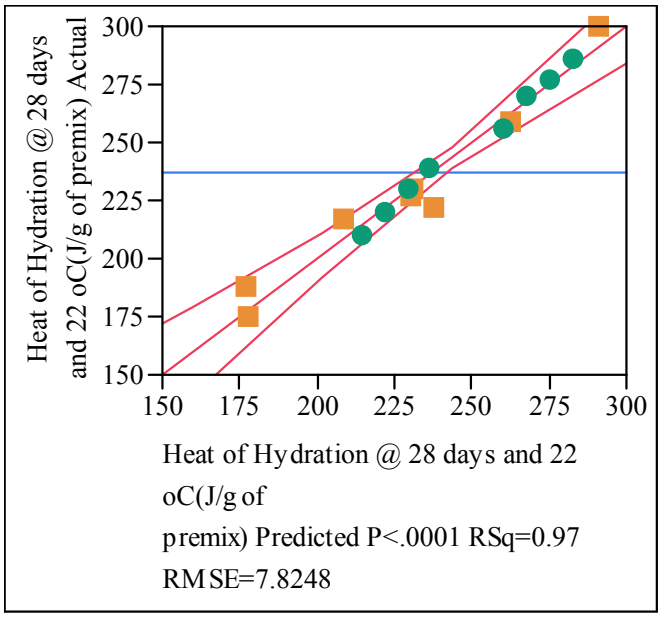

Figure 3-17 Actual vs. predicted values of heat of hydration for samples of Phases 8 and 9 measured at 25 °C only. The green circles are data from phase 9 mixes and the orange squares from phase 8 mixes

The model (equation) for prediction of heat of hydration (HOH) expressed in J/g of premix, where [ ] indicates Molarity and T is the temperature in °C, is:

$$HOH = -85.5 + 147.8 \cdot w/cm + 3.1 \cdot wt\ \%\ slag + 14.0 \cdot [OH^-] + 160.0 \cdot [aluminate] - 9.3\ phase$$

The R^2 for this fit is 97 % and identifies w/cm ratio, wt % slag, free hydroxide and aluminate as significant drivers of the heat of hydration of the Saltstone mixes. In this case, a phase difference between phases 8 and 9 was also observed and is unexplained. It accounts for 9.3 J/g of premix with Phase 9 showing higher heat of hydration than Phase 8.

3.10 Observation of Cracking for Mixes Containing 0.44 M Aluminate

The time dependencies of Young's modulus for the Phase 8 samples cured at 22 °C were measured and are reported in Table 3-6. An interesting observation was noted for four of the 10 samples at 90 days. No signals could be obtained from these samples using the resonance frequency system to measure E due to the fact that the samples had cracked. One common factor for these four samples is a maximum level of aluminate of 0.44 M in the salt solutions used to batch these mixes. Figure 3-18 is a photograph that shows the longitudinal crack that extends the entire length of the cylinder with a depth of ~ 3 cm based on the crack length on the top and bottom of the cylinders. The other factor that is common to all four samples is the temperature of curing which remained constant at 22 °C. Samples cured under these conditions continue to develop strength as hydration reactions continue to occur. This is not the case for samples

subjected to higher curing temperatures initially where continued strength development is not observed.

Table 3-6 Young's Modulus as a Function of Time for Four Samples from Phase 8

Cure Temp	Sample ID	Young's Modulus in GPa			
°C		14 days	28 days	56 days	90 days
22	GVS 91	10.5	11.5	12.7	cracked
22	GVS 93	8.6	9.4	10.3	cracked
22	GVS 94	9.2	9.5	10.0	cracked
22	GVS 95	11.2	11.7	11.1	cracked

Figure 3-18 Photo of GVS 91 after 90 days of curing showing the longitudinal crack the entire length of the 6 inch long cylinder

4.0 CONCLUSIONS

The results demonstrate that performance properties as well as some of the processing properties of Saltstone are highly sensitive to the conditions of time and temperature under which curing occurs. This sensitivity is in turn dependent on the concentration of aluminate in the salt feed solution. In general, the performance properties and indicators (Young's modulus, compressive strength and total porosity) are reduced when curing is carried out under high temperature initially. However, this reduction in performance properties is dependent on the sequence of temperatures (the time/temperature profile) experienced during the curing process. That is, samples that are subjected to a 1, 2, 3 or 4 day curing time at 60 °C followed by final curing at 22 °C lead to performance properties that are significantly different than the properties of grouts allowed to cure for 1, 2, 3 or 4 days at 22 °C followed by a treatment of several days at 60 °C. The performance properties of Saltstone cured in the sequence of higher temperature first are generally less (and in some cases significantly less) than performance properties of Saltstone cured only at 22 °C. This loss in performance was shown to be mitigated by increased slag content and/or cement content in the premix at the expense of fly ash. For the sequence in which the Saltstone is cured initially at 22 °C followed by a higher temperature cure, the performance properties can be equal to or greater than the properties observed with only 22 °C curing. The results in this report indicate that in order to meaningfully measure and report the performance properties of Saltstone, one has to know the time/temperature profile conditions under which the Saltstone will be cured.

These results can be explained in general by assuming that structure of the CSH gel formed initially with a 22 °C curing temperature is different than the structure of the CSH gel formed at higher temperatures [8]. The CSH gel at room temperature can continue to hydrate and strengthen at both room temperature and higher curing temperatures. Conversely, the CSH gel formed at higher temperatures is resistant to further hydration at any temperature. For example, the outer layer of the CSH particles formed at higher temperatures may have low solubility and diffusivity and therefore preclude the dissolution and diffusion necessary for additional hydration reactions to occur. Further characterization of the microstructures of Saltstone cured under different temperatures is required to confirm this assumption.

Aluminate concentrations at levels greater than 0.20 M in these salt solutions lead to both positive and negative effects on the performance properties. At a curing temperature of 22 °C, aluminate increases Young's modulus and the compressive strength while reducing the total porosity. This generally corresponds to an improved permeability (hydraulic conductivity) for Saltstone which is a positive outcome. However, there is a significant increase in heat of hydration with increased aluminate concentration that may limit pour schedule and must be considered in estimating the time/temperature profile to which Saltstone will be subjected during curing as discussed above. That is, higher temperatures in the vault (due to the higher heats of hydration) may present a greater challenge in controlling the curing time and temperature profile to achieve the desired performance properties.

The results of this study demonstrate that decreasing the w/cm ratio or increasing the slag content of the premix increases the performance properties of Saltstone. Predictive models were

generated for these higher aluminate Salt Waste Processing Facility (SWPF) mixes that identify the important parameters that control Young's modulus, porosity and heat of hydration. These parameters include w/cm ratio, slag content, temperature, and aluminate, nitrate, nitrite and free hydroxide concentrations in the salt solutions. These models and data sets will serve as the basis to which new data from future batches can be added that in turn allow for a revision to the models with the expanded parameter ranges.

The heat of hydration measurements for these mixes demonstrated that aluminate and higher slag content (at the expense of fly ash) increase the total heat output and result in projected adiabatic temperature increases between 70 °C to 85 °C. The actual temperature increase in the vaults will be less than this due to heat losses which can be predicted by thermal modeling.

The results on total porosity and Young' s modulus for the mixes of Phases 8 and 9 at various cure temperatures were added to the existing data set for these properties and regressed linearly to determine whether a correlation exists. In fact, a linear correlation does exist with a R^2 of 80 % with some additional structure observed within the plot. In general, permeability (which is the input to the Performance Assessment modeling) is correlated with porosity so, a demonstration of a correlation between porosity and Young's modulus provides confidence in the use of Young's modulus as a performance indicator. Independent measurements are underway in an attempt to correlate permeability with Young's modulus directly.

An interesting observation was the presence of longitudinal cracks over the entire length of the 14 cm cylinders after long curing times (first noticed at 90 days for the Phase 8 samples at the time of measurement of Young's modulus). The common parameters for the four samples that cracked were the maximum concentration of aluminate (0.44 M) and curing at 22 °C. As discussed above, samples cured at 22 °C continue to hydrate which in this case leads to cracking.

5.0 PATH FORWARD

The results in this report indicate that in order to meaningfully measure the performance properties of Saltstone, one has to know the time/temperature profile conditions under which the Saltstone will be cured. This will require thermal modeling and/or actual time/temperature profiles within the vaults under various pour schedules to determine (1) an average profile of time and temperature under normal processing and (2) a conservative (worst case) profile. Samples can then be cast and cured in the laboratory under these time and temperature profiles prior to measurement of the performance properties of the product waste forms.

It is important to measure the heat of hydration at 40 °C and 60 °C for these mixes. This will determine whether the reduced performance properties developed under the time and temperature curing profiles are due to a lower degree of hydration or due to the development of a distinctly different CSH gel structure at higher temperature. In any event, it is important to know the total heat of hydration at higher temperatures since this will impact the modeling of temperature profile and pour schedule in the vaults.

6.0 REFERENCES

[1] *Effect of Increased Aluminate Concentrations on Saltstone Mixes,* J. R. Harbour, T. B. Edwards, E. K. Hansen and V. J. Williams, WSRC-STI-2007-00506, Rev. 0, 2007.

[2] *Memo Report on the Subtasks for the Saltstone Variability Study for 2009*, J. R. Harbour and T. B. Edwards, SRNL L3100-2008-00048, October 2008.

[3] *Scoping Studies for Development of Saltstone Variability Study*, J. R. Harbour and T. B. Edwards, WSRC-RP-2005-01439, Rev. 0, 2005.

[4] *Heat of Hydration of Saltstone Mixes – Measurement by Isothermal Calorimetry*, J. R. Harbour, V. J. Williams and T. B. Edwards, WSRC-STI-2007-00263, Rev. 0, 2007.

[5] *Saltstone Performance Indicator*, J. R. Harbour and V. J. Williams, SRNL-STI-2008-00488, Rev. 0, December 2008.

[6] *Saltstone Variability Study –Measurement of Porosity,* J.R. Harbour, V.J. Williams, T.B. Edwards, R.E. Eibling, and R.F. Schumacher, WSRC-STI-2007-00352, Rev. 0.

[7] *Variability Study for Saltstone*, J. R. Harbour, T. B. Edwards, E. K. Hansen and V. J. Williams, WSRC-TR-2005-00447, October 2005.

[8] *Cement Chemistry*, H. R. W. Taylor, Thomas Telford Publishing, 1997.

[9] *Permeability of Saltstone*, J. R. Harbour, T. B. Edwards, V. J. Williams, D. M. Feliciano and G. W. Scherer WSRC-STI-2007-00437, Rev. 0, 2007.